

# Comparison of vibration and rolling noise emission of resilient and solid monobloc railway wheels in underground lines

*B. Suarez, B. J. Serrano, P. Rodriguez, J. Blanquer*

Flat or worn wheels rolling on rough or corrugated tracks can provoke airborne noise and ground-borne vibration, which can be a serious concern for nearby neighbours of urban rail transit lines. Among the various treatments used to reduce vibration and noise, resilient wheels play an important role. In conventional resilient wheels, a slightly prestressed V-shaped rubber ring is mounted between the steel wheel centre and tyre. The elastic layer enhances rolling noise and vibration suppression, as well as impact reduction on the track. In this paper the effectiveness of resilient wheels in underground lines, in comparison to monobloc ones, is assessed. The analysed resilient wheel is able to carry greater loads than standard resilient wheels used for light vehicles. It also presents a greater radial resiliency and a higher axial stiffness than conventional V-wheels. The finite element method was used in this study. A quarter car model was defined, in which the wheelset was modelled as an elastic body. Several simulations were performed in order to assess the vibrational behaviour of elastic wheels, including modal, harmonic and random vibration analysis, the latter allowing the introduction of realistic vertical track irregularities, as well as the influence of the running speed. Due to numerical problems some simplifications were needed. Parametric variations were also performed, in which the sensitivity of the whole system to variations of rubber prestress and Poisson's ratio of the elastic material was assessed. Results are presented in the frequency domain, showing a better performance of the resilient wheels for frequencies over 200 Hz. This result reveals the ability of the analyzed design to mitigate rolling noise, but not structural vibrations, which are primarily found in the lower frequency range.

*The final, definitive version of this paper has been published in Proceedings of the 7th World Congress on Railway Research, Montréal, Canada, 4-8 June, 2006.*

*When citing this work, please refer to the published paper:*

*B. Suarez, B. J. Serrano, P. Rodriguez, J. Blanquer, Comparison of vibration and rolling noise emission of resilient and solid monobloc railway wheels in underground lines. Proceedings of the 7th World Congress on Railway Research, Montréal, Canada, 4-8 June, 2006.*

## Comparison of vibration and rolling noise emission of resilient and solid monobloc railway wheels in underground lines

B. Suarez<sup>1</sup>, B. J. Serrano<sup>1</sup>, P. Rodriguez<sup>1</sup>, J. Blanquer<sup>2</sup>

<sup>1</sup>Railway Technologies Research Centre, Madrid, Spain, <sup>2</sup>Metro de Madrid, Madrid, Spain

### Abstract

Flat or worn wheels rolling on rough or corrugated tracks can provoke airborne noise and ground-borne vibration, which can be a serious concern for nearby neighbours of urban rail transit lines. Among the various treatments used to reduce vibration and noise, resilient wheels play an important role.

In conventional resilient wheels, a slightly prestressed V-shaped rubber ring is mounted between the steel wheel centre and tyre. The elastic layer enhances rolling noise and vibration suppression, as well as impact reduction on the track.

In this paper the effectiveness of resilient wheels in underground lines, in comparison to monobloc ones, is assessed. The analysed resilient wheel is able to carry greater loads than standard resilient wheels used for light vehicles. It also presents a greater radial resiliency and a higher axial stiffness than conventional V-wheels.

The finite element method was used in this study. A quarter car model was defined, in which the wheelset was modelled as an elastic body. Several simulations were performed in order to assess the vibrational behaviour of elastic wheels, including modal, harmonic and random vibration analysis, the latter allowing the introduction of realistic vertical track irregularities, as well as the influence of the running speed. Due to numerical problems some simplifications were needed. Parametric variations were also performed, in which the sensitivity of the whole system to variations of rubber prestress and Poisson's ratio of the elastic material was assessed.

Results are presented in the frequency domain, showing a better performance of the resilient wheels for frequencies over 200 Hz. This result reveals the ability of the analyzed design to mitigate rolling noise, but not structural vibrations, which are primarily found in the lower frequency range.

### 1. Introduction

#### Resilient wheels features

Flat or worn wheels rolling on rough or corrugated tracks can provoke airborne noise and ground-borne vibration, which can be a serious problem for buildings and residents close to urban rail transit lines [6]. Among the various treatments used to reduce vibration and noise, resilient wheels play an important role.

In conventional resilient wheels, a slightly prestressed V-shaped rubber ring is mounted between the steel wheel centre and tyre [9]. The elastic layer enhances rolling noise and vibration suppression, as well as impact reduction on the track. It also softens the elastic transmission of traction and braking forces and reduces wheel and rail wear, thus increasing the service life of the tyre. These characteristics make resilient wheels especially suitable for use on intensively-used urban and suburban mass transport.

Being initially designed for light rail systems, such as trams [1], in order to reduce rolling noise on tangent track and wheel squeal on tight curves [11], they have been intensively used for years with apparently satisfactory results.

Although resilient wheels are rarely found on mainlines, when first noise problems arose on early ICE trains, resilient wheels inspired by light rail replaced the original monobloc ones [2, 8]. The noise problems were reduced, but the strain on the wheel rims increased, finally causing the disintegration of a tyre in the summer of 1998. This was the origin of a tragic sequence of unfortunate circumstances causing the Eschede (Germany) accident [4, 7]. This accident stroke a great blow for resilient wheels to be mounted on high speed trains. As a

consequence, very few research works have been published regarding resilient wheels effectiveness, despite thousands of them are still in operation for urban transport, without any noticeable incident.

### Comparative study

In a cooperation project between the Railway Technologies Research Centre (CITEF) of the Polytechnic University of Madrid (UPM), and Metro de Madrid, the effectiveness of resilient wheels specifically designed for underground lines, in comparison with monobloc ones, was assessed. The analysed resilient wheel, which is equipped with a V-shaped rubber ring, is able to carry greater loads than those mounted on light vehicles. It also presents a greater radial resiliency and a higher axial stiffness than conventional V-wheels.

The finite element method was used in this study. A quarter car model has been defined in the Ansys program, in which the wheelset was modelled as an elastic body. Several simulations were performed in order to assess the vibrational behaviour of elastic wheels, including modal, harmonic and random vibration analysis, the latter allowing the introduction of realistic vertical track irregularities, as well as the influence of running speed.

## 2. Description of the analysed wheel

The wheel comprises a wheel centre and a flanged tyre, both made of steel, a rubber ring and a steel pressure ring (see Figure 1) [10].

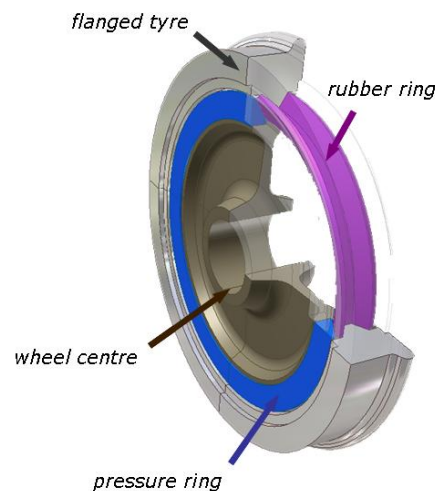


Figure 1: Resilient wheel components

- The rubber ring has an V-shaped section, whose flanges form an angle of  $60^\circ$  with the wheel axis, thus providing a greater resiliency in the radial direction and a better stiffness in the axial direction than other conventional resilient wheels. The rubber ring does not completely fill the space designated for it between the steel parts, and usually only the rubber ring flanges transmit loads (they are exposed to shear and pressure). For higher loads, the central part of the annular body is also transmitting pressure loads, thus giving the wheel a progressive stiffness increase.
- The pressure ring is attached to the wheel centre by screw joints, which squeeze the rubber ring and ensure a permanent contact between the rubber ring and the surrounding steel pieces.
- The steel components are provided with annular grooves in the surfaces that come in contact with the rubber ring, increasing the contact surface and preventing undesired circumferential movements of the rubber ring.

## 3. Simulation models

### General features

Quarter car models were set up (including a wheelset, a half bogie and a quarter carbody) in order to compare the dynamic behaviour of resilient and monobloc wheels.

The wheelset was modelled with the finite element technique. A lumped mass was also placed on the wheelset axis, in order to consider the influence of the brake disc. The bogie and the carbody were treated as rigid bodies. Wheelset, bogie and carbody were joined by the springs of the primary and secondary suspension.

#### Wheelset meshing

In the finite element model, the wheel geometry was simplified, even though the principal features of both wheelset and axis were maintained. The annular grooves of the resilient wheel, which prevent undesired circumferential movements between rubber and steel pieces, were replaced by movement constraints between nodes in both surfaces.

After simplifying the geometry, a half section of the axis and the wheel were meshed, using plane square elements. The resilient wheel was meshed using smaller elements for the rubber component, subjected to higher deformations. Then the plane mesh was revolved around the axis of symmetry, thus obtaining a three-dimensional model composed by hexahedral elements (SOLID45) (Figure 2).

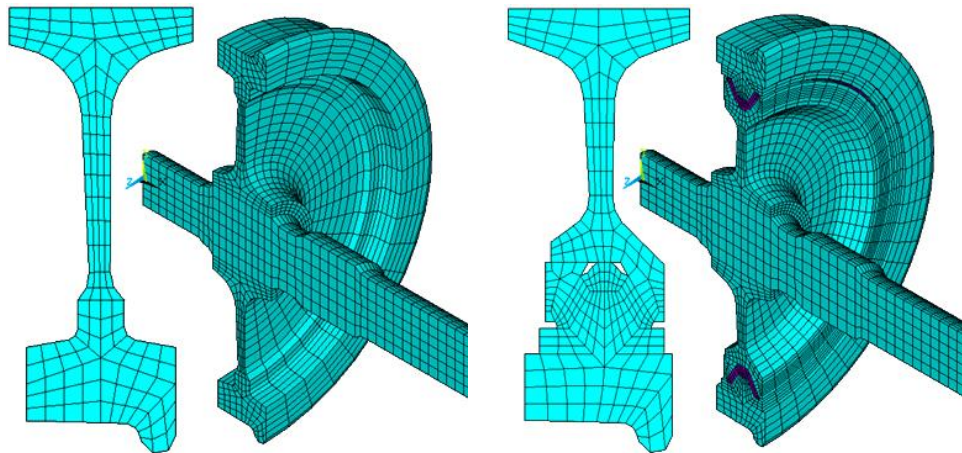


Figure 2: Wheel and axis meshing: monobloc (left) and resilient (right) wheels

Hyperelastic elements are usually used when modelling rubber materials, that have Poisson's ratios close to 0.5. These elements are based on a mixed non-linear pressure-displacement (p-U) formulation, which only can be used for static or transitory analyses. However, harmonic and power spectral density analyses seem to be more suitable to assess the dynamic behaviour of the vehicle. Since the later analyses are based on a previous modal one, intrinsically linear, and the rubber ring deformations are small, the rubber part was meshed using solid elements with linear characteristics (SOLID45).

#### Boundary conditions

The study focused on the main external source of vibration, which are the track vertical irregularities. Thus, symmetry boundary conditions could be applied to the vertical plane which contains the rolling axis, in order to reduce computation time. For the same reason, only vertical and roll movements of the bogie and the carbody were allowed.

The contact between the wheel and the rail, where the excitation due to the track irregularities is applied, was modelled by vertical constraints defined on both wheels, at the contact point location.

#### Rubber ring prestress

In its steady state, the rubber ring is prestressed. This compression causes a permanent tensional state, affecting the rubber stiffness and, therefore, the resilient wheel dynamics. In order to take into account this effect, a previous static analysis was performed, in which the rubber was compressed, and its initial stress state was modified.

In the starting model, the rubber ring had no initial deformation. Initially, the pressure ring was axially displaced outwards from its final position, until coming into contact with the outer side of the undeformed rubber ring (Figure 3, left). This initial displacement of the pressure ring was computed according to the real interference between the steel and rubber components in the final stage of the assemblage process, but had opposite

direction. The wheel tyre was completely attached to the rubber ring, whilst the wheel centre and the pressure ring were only connected to the rubber flanges, but not to the central part of the rubber ring (attachment nodes are marked with green crosses in Figure 3). All the wheel centre degrees of freedom were constrained, and an axial displacement was imposed to the external face of the pressure ring, forcing it to move towards its final position.

The resulting stresses obtained in the static analysis were stored as the initial state for further dynamic analysis. Node positions were also updated, and finally the wheel centre and the pressure ring were attached to the rubber ring (Figure 3, right). When defining the mesh size, the final position of the nodes had to be considered, so that they could be joined after the aforementioned static calculation.

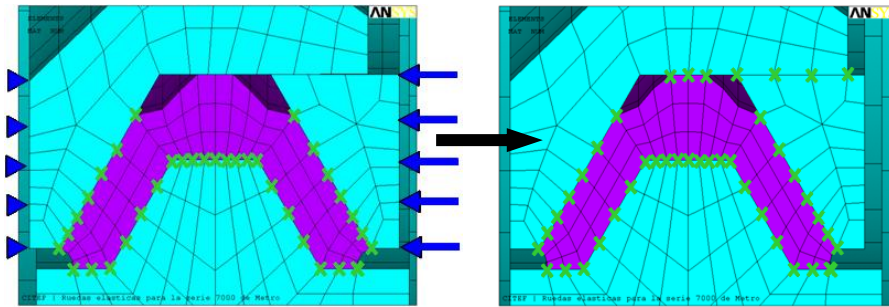


Figure 3: Rubber ring prestress: initial state (left) and final state (right)

#### Loads applied to the wheelset

Track irregularities are transmitted to the wheelset through the wheel-rail contact patch, and from here to the rest of the vehicle, through the primary and secondary suspensions.

To apply a movement constraint over a wheel area of the same size as the real contact patch (around  $3 \text{ cm}^2$ ), a very thin mesh would be required, thus increasing computation time. On the other hand, if the original mesh size was maintained in this area, the constraint would affect only a single node, thus causing high local unrealistic deformations. In order to avoid these inconveniences, a small area around the theoretical contact point was stiffened, and the movement constraint was applied to an additional node, rigidly attached to this area. In this manner, all nodes pertaining to the stiffened area shared the same displacement.

A similar problem appeared in those points where the wheelset extremes were attached to the primary suspension springs. In order to avoid this problem, the spring end was attached to a special node that was joined to all the nodes belonging to the bearing supporting surface, thus proportionally distributing the received force between them.

The weight of the disk brake was transmitted in the same manner to all the nodes belonging to the wheelset surface where the disc is mounted.

#### **4. Preliminary studies**

Some limitations for the resilient wheel model were found when using linear elements in the rubber mesh with a Poisson's ratio of 0.48 (almost no compressibility at all). The low compressibility led to erroneous solutions when the rubber ring was compressed more than a certain limit value. For this reason, the influence of Poisson's ratio and the initial rubber compression on the final results was analysed. Lower, admissible values for the Poisson's ratio were found that did not noticeably affect the final results.

By means of a sensitivity study, the frequency response of the system was compared for different values of the Poisson's ratio and of the interference existing between the rubber and the steel pieces, under a sinusoidal vertical excitation applied to the wheel, in the frequency range between 0 and 200 Hz.

The graphs shown in Figure 4 correspond to the frequency response functions obtained for the vertical displacement of the wheelset's extreme end, for Poisson's ratios of 0.48 (actual value), 0.5 and 0.4, and interferences of 1 (actual value), 0.7, 0.4 and 0 mm. As the Poisson's ratio decreases, higher interferences can be applied to the rubber material. The rubber ring that allows a higher interference and thus higher initial prestress without leading to erroneous results is that of Poisson's ratio equal to 0.4.

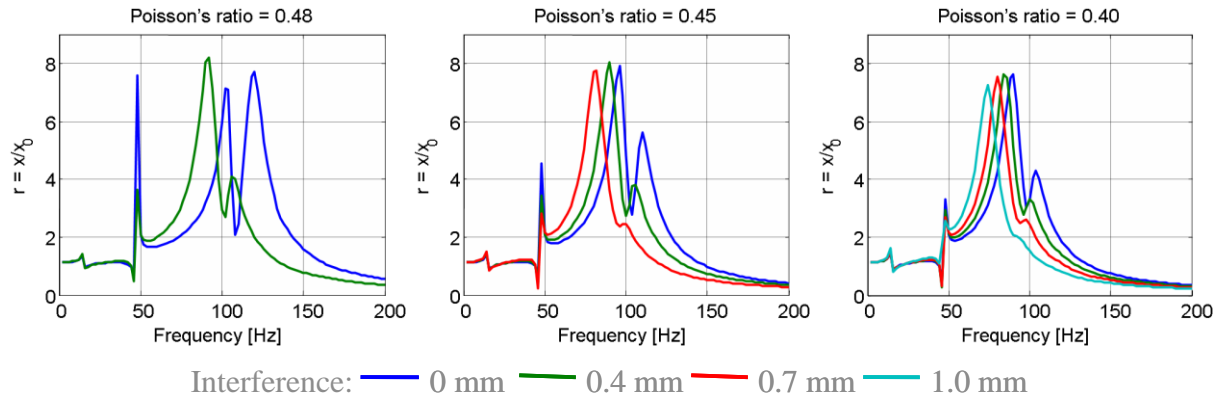


Figure 4: Frequency response function for diverse Poisson's ratios and geometric interferences

In the comparative study shown in Figure 4, the obtained curves revealed a higher difference in the frequency range between 50 and 140 Hz. In this range, resonance of the rubber ring and the second bending mode of the wheelset, in which the rubber has a great displacement, occurred.

It could be seen that, when lowering Poisson's ratio, the peaks were shifted to the left, whilst, when lowering the geometric interference, peaks moved to the right, thus balancing the previous effect. However, it was also observed that, when increasing the geometrical interference, the differences between rubber materials with different Poisson's ratios were reduced. In any case, the observed differences between the cases studied were of relatively small importance.

According to these results, the model which was closest to reality was that allowing the higher possible geometric interference, even though Poisson's ratio was smaller than the real value. In the definitive models a geometric interference of 0.9 and a Poisson's ratio of 0.4 were defined, being a good enough approximation to reality.

## 5. Modal analysis

Table 1 shows the first eigenfrequencies for vehicle models with resilient and monobloc wheels. Differences between both models were noticed from the sixth mode on.

<u>Monobloc Wheels</u>			<u>Resilient Wheels</u>		
Mode	Description	Freq. [Hz]	Mode	Description	Freq. [Hz]
1	Carbody roll	0.94	1	Carbody roll	0.94
2	Carbody vertical displ.	1.25	2	Carbody vertical displ.	1.25
3	Bogie roll	15.28	3	Bogie roll	14.82
4	Bogie vertical displ.	15.64	4	Bogie vertical displ.	15.35
5	Wheelset 1 <sup>st</sup> bending mode	49.77	5	Wheelset 1 <sup>st</sup> bending mode	46.50
6	Wheelset 2 <sup>nd</sup> bending mode	116.4	6	Left rubber ring resonance	76.68
7	Wheelset 3 <sup>rd</sup> bending mode	143.8	7	Wheelset 2 <sup>nd</sup> bending mode	92.66
8	Symmetric umbrella	216.6	8	Wheelset 3 <sup>rd</sup> bending mode	112.9
9	Anti-symmetric umbrella	293.7	9	Right rubber ring resonance	135.1
			10	Symmetric umbrella	145.1
			11	Anti-symmetric umbrella	192.2
			12	Bending of left wheel tyre	274.4

Table 1: Eigenfrequencies of models with monobloc (left) and resilient (right) wheels

## 6. Harmonic analysis

When running over a track at a given velocity, rail geometric irregularities are transformed into a time excitation applied on the vehicle at the contact point. On the other hand, the own motion of the wheelset is transmitted to

the track through the contact point and to both bogie and carbody through the primary and secondary suspensions. Noise is also emitted.

During the harmonic analysis, a vertical sinusoidal displacement was applied at the wheel contact patch, having a constant amplitude and a variable frequency in the range between 0 and 1000 Hz.

### Results

The system response was obtained in several representative points on the wheelset, the bogie and the carbody. Frequency response functions give the ratio between the response obtained at a certain point and the applied excitation, for all the frequencies considered. As an example, Figure 5 shows the frequency response functions for the force transmitted to the rail, for wheelsets with both monobloc and resilient wheels.

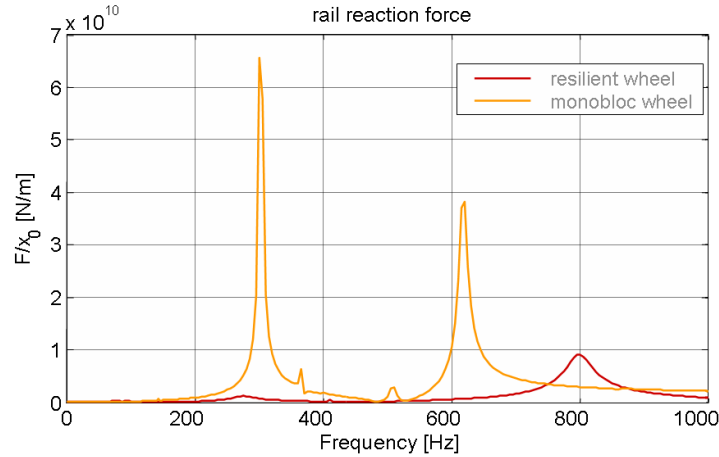


Figure 5: Rail reaction force

As can be seen, for frequencies higher than 150 Hz, resilient wheels revealed a noticeably better behaviour.

## 7. Power spectral density analysis

In order to evaluate the effect that stochastic vibrations induce on the system, rail-specific power spectral density (PSD) functions, defining track irregularities, are usually employed, which put a great emphasis on longer wavelengths than on shorter ones. Short wavelength defects (from 20 cm to 3 m) are related to the rail shape and the rail's welding joints, while medium (from 3 to 25 m) and long (greater than 25 m) wavelengths are associated to geometrical defects of the ballast layer and platform [5].

In this study, the effect of the resilient wheel running on a slab track was of concern. Therefore, it was considered that the contribution of medium and long wavelength irregularities, related to the presence of ballast layer, was small. To define vertical irregularities, a PSD function published by the ERRI B176 committee [3] was used. This PSD function is representative of a track with a low vertical irregularity level and is given by:

$$S_z = A_z \frac{\Omega^2 C}{\left( \Omega^2 + \Omega_R^2 \right) \left( \Omega^2 + \Omega_C^2 \right)}$$

with  $\Omega_C = 0.8246$  rad/m,  $\Omega_R = 0.0206$  rad/m and  $A_z = 4.032 \cdot 10^{-7}$  m·rad, being  $\Omega$  the spatial frequency.

When running on the track, the vehicle wheels pass over the rail irregularities at a certain speed, so that the track spatial irregularities  $z(s)$  are converted into time excitations  $z(t)$  acting on the wheels. The relationship between the time PSD,  $S_z(\omega)$ , acting on the wheel and the spatial PSD,  $S_z(\Omega)$ , due to the track irregularities, are related by the vehicle velocity,  $V$ :

$$S_z(\omega) = \frac{1}{V} S_z(\Omega)$$

For this study, a running speed of 70 km/h was considered.

On railway tracks, the maximum wavelength is usually found up to 100 m. This maximum wavelength corresponds to a minimum frequency of 0.2 Hz for running velocities of 70 km/h. On the opposite end, a track excitation over 1000 Hz is considered negligible, even though the audio spectrum reaches higher values. Therefore, in order to analyse the system's effectiveness on reducing noise emission, its response was computed for frequencies up to 1000 Hz. For a running velocity of 70 km/h, frequencies up to 1000 Hz correspond to wavelengths over 0.02 m.

Given the transfer function  $H_z(\omega)$  at a certain point, its PSD response can be computed according to the following relationship:

$$S_z(\omega) = |H_z(\omega)|^2 \cdot S_z(\omega)$$

To compute the PSD functions for the vehicle response, the transfer functions obtained in the previous harmonic analysis were used.

### Results

As an example, Figure 6 shows the response PSD obtained for the vertical displacement of two different points, located at the wheelset centre and on top of the wheel, for wheelsets with both resilient and monobloc wheels.

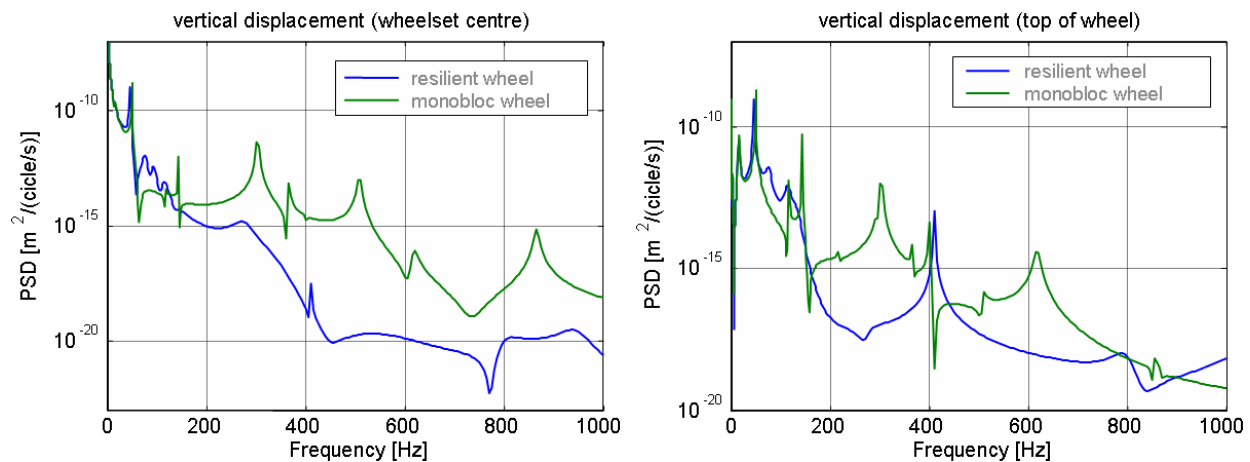


Figure 6: Vertical displacements for points located at the wheelset centre (left) and top of the wheel (right)

The excitation used in harmonic analyses has the same magnitude over all frequencies, whilst the excitation used in PSD analyses has lower amplitudes for higher frequencies. However, From a qualitative point of view, the system response obtained in the PSD analysis reveal the same tendency than frequency response functions computed during harmonic analysis, and the same kind of observations were made.

## 8. Summary of the results obtained in this study

Additional results were obtained for other points on the quarter car model, but had not been included graphically in this paper. The following results were observed:

**Carbody and bogie responses:** The carbody and the bogie oscillated with almost the same vertical displacement as the excitation, for frequencies lower than their own vertical eigenfrequencies (1 Hz for the carbody and 15 Hz for the bogie). Close to those frequencies, the displacements reached their maximum values. For higher frequencies, the vibrations were mainly absorbed by the suspensions, thus having very small displacements. This effect was emphasized in the PSD analysis.

**Wheelset response:** The responses at different representative points on the wheelset were obtained in order to study the wheelset's vertical vibrations. For all points, it was observed that: for lower frequencies (up to 45 Hz), models with resilient and monobloc wheels showed a similar behaviour; for frequencies between 45 and 200 Hz, models with resilient wheels showed a worse dynamic behaviour, due to the resonances of the rubber rings,



which were found in this range; for frequencies over 200 Hz, the vertical vibrations of the model with resilient wheels were very much lower than those of the model with monobloc wheels, as can be seen in Figure 6.

In the high frequency range, in which resilient wheels revealed a better behaviour than monobloc ones, the PSD function of track irregularities was rather small, and so was the system's response. However, this frequency range was large enough to let the area below the curve be greater than the one for lower frequencies, where the resilient wheel had a worse behaviour. Therefore, it can be stated that resilient wheels are more suitable for reducing both the transmission of vibrations to the carbody and the noise emission.

Rail reaction forces: As for the vertical displacements, the forces transmitted to the rail were similar for both models, in the frequency range up to 50 Hz, whilst for frequencies higher than 150 Hz the models with resilient wheels revealed a noticeably better behaviour.

The main part of the vibrations transmitted to neighboring structures takes place at frequencies below 100 Hz [5]. At higher frequencies, these vibrations are quickly damped, being this effect of higher importance as the frequency rises. On the contrary, the energy related to higher frequencies (between 30 and 2000 Hz) is radiated as noise from the wheels and rails. Having in mind these considerations, it can be stated that resilient wheels are effective for noise reduction, although they seem not to be very useful when mitigating structural vibrations.

## 9. Conclusions

Several simulations were performed in order to assess the vibrational behaviour of elastic wheels, including modal, frequency response and random vibration analysis, the latter allowing the introduction of realistic vertical track irregularities, as well as the effect of running speed. Parametric variations were also performed, assessing the sensitivity of the whole system to variations of rubber prestress and Poisson's ratio of the elastic material.

Results are presented in the frequency domain, showing a better performance of the resilient wheels for frequencies over 200 Hz. This result reveals the ability of the analyzed design to mitigate rolling noise, but not structural vibrations, which are primarily found in the lower frequency range.

In case that the transmission of vibrations to the neighbouring structures was subject to being reduced, a different kind of mitigation system should be chosen. Usually, such systems are mounted on the track, and not on the rolling stock.

## Acknowledgements

The authors gratefully thank Metro de Madrid for funding and supporting the present study.

## References

- [1] P. Bouvet and N. Vincent. "Optimization of Resilient Wheels for Rolling Noise Control", *Journal of Sound and Vibration*, Vol. 231, pp. 765-777 (2000).
- [2] H. Claus. "On Dynamics of Radialelastic Railway Wheelsets", *Proc. VSDIA'2000*, (Budapest, 6-8 November 2000), pp. 263-270 (2000).
- [3] ERRI DT 290 B 176. "Bogies with Steered or Steering Wheelsets. Technical Document dt 290. Benchmark Problem. Results and Assessment".
- [4] V. Esslinger, R. Kieselbach, R. Koller, B. Weisse. "The Railway Accident of Eschede – Technical Background", *Engineering Failure Analysis (SCI)*, Issue 11, pp. 515-535 (2004).
- [5] C. Esveld. "Modern Railway Track", Second Edition, *MRT-Productions*, ISBN 90-800324-3-3 (2001).
- [6] Harris Miller Miller & Hanson Inc. "Transit Noise and Vibration Impact Assessment: Final Report", chapter 7 (1995).
- [7] G. J. Kuepper. "High-Speed Crash Kills 101", *NFPA Journal*, Vol. 93 No. 6 (Nov/Dec), pp. 40-44 (1999).
- [8] Krupp Stahl AG. "Rail wheel with rubber suspension", *Patent DE3328321* (1985).
- [9] Patent Products Limited. "Wheels Having a Hub and a Metal Rim", *Patent GB895520* (1962).
- [10] SAB Wabco. "A Rail Vehicle Wheel", *Patent EP 489 455 B1* (1992).
- [11] Wilson, Ihrig & Associates, Inc. "Wheel and Rail Vibration Absorber Testing and Demonstration", *TCRP Report 67* (2001).